oi: 10.18178/ijges.7.1.1-8

Nature and Source of the Ore-forming Fluids Characterisation of Gadag Schist Belt, Dharwar Craton using Geochemistry and Fluid Inclusion Studies

Girish Kumar M[1], Korakoppa, M, M[1], Kalyana Krishna[1], Madhushree Mondal[2] and Ajit Singh[3]
[1]National Centre for Excellence in Geoscience Research, Remote Sensing and Aerial Survey, Geological Survey of India, Bangalore, India
[2]National Centre for Excellence in Geoscience Research, Geological Survey of India, Faridabad, India
[3]Remote Sensing and Aerial Survey, Geological Survey of India, Bangalore, India
Email: girishgeosu@gmail.com

***Abstract*—Gadag Schist Belt (GSB) is the northern continuity of Chitradurga Schist Belt (CSB) of Archean age (~ 2600 Ma). The GSB comprises of metavolcanics and metasediments and are surrounded by older TTG and younger granitoids. The gold mineralisation is confined to quartz veins hosted by metabasalt and metasedimentary and also associated with wall rock alteration (carbonitisation, chloritisation and seritisation). EPMA studies confirmed the gold association with pyrites. The analysis of the gold grain (3 to 6 micron) associated within the pyrite grain, the Au content varies from 84.64 to 82.64 wt. % and Ag content from 4.84 to 9.74 wt. % and other sulphides. The REE patterns shows enriched in LREE and depleted in HREE patterns, but with positive Eu anomaly indicates the hydrothermal fluids responsible for wall rock alterations and particularly LREE from host metabasalts or metasedimentory rocks. Fluid inclusion microthermometry in auriferous quartz veins reveal the existence of a metamorphogenic aqueous–gaseous (H_2O–CO_2–CH_4+Salt) fluid that underwent phase separation and gave rise to gaseous (CO_2–CH_4), low saline (~5 wt.% NaCl equiv.) aqueous fluids. The estimated P–T range (240 to 360°C and 1.0 to 2.0 Kbar) compare well with the published P–T values of other orogenic gold deposits in general, considerable pressure fluctuation characterize gold mineralization at GSB. Ore fluids of the GSB with other gold deposits in the Dharwar Craton, confirms that fluids of low saline and aqueous–carbonic composition with metamorphic parentage played the dominant role in formation of Archean lode gold systems.**

***Index Terms*—gadag, fluid inclusion, gold, dharwar craton.**

I. Introduction

Archean lode gold deposits are associated with range of meta-volcanics to meta-sediments to granitoid plutons. Nature and composition of ore fluids associated with Archean lode gold deposits has been developed from a wide range of studies related to fluid inclusions, stable/radiogenic isotopes, REE and geochemistry of hydrothermally altered rocks. Numerous studies, reviews that the ore fluids are consistently neutral to weakly alkaline, low to moderate salinity aqueous – gaseous fluids with high CO_2 ($\pm CH_4$) even, when the deposits ranged from sub-greenschist to upper-amphibolite facies metamorphic conditions. Hence, the characteristic ore fluid associated with the Archean gold deposits is well accepted to be a low salinity fluid capable of carrying Au as well as Ag, As and Sb but with inadequate capacity to transport base metals (Ridley and Diamond, 2000) Ref. [1].

Understanding the origin of auriferous hydrothermal fluids Goldfarb and Groves (2015) have summarized the nature of ore-forming fluids in orogenic gold deposits are metamorphic devolatilization during prograde regional metamorphism of the greenstones and devolatilization of the lower and/or middle crust with or without input from the mantle (Kerrich, 1991; Groves *et al.*, 2003) Ref. [2,3]. Metamorphism of the greenstones has been examined by Kolb *et al.* (2004) Ref. [4]. Low-salinity (3.9–13.5 wt % NaCl equ.) aqueous inclusions, characteristic of orogenic gold deposits and were coexist with carbonic ($CO_2 \pm CH_4$) inclusions at pressures and temperatures of 1.0 to1.7 kbars and 280 to 320°C in the gold mineralised quartz veins at Hutti (Pal and Mishra, 2002).

Detailed geology and gold deposits of GSB was given by Maclaren (1906) and Narayanaswami (1959) gave a complete account of the old mines in the Gadag Gold Fields and Mohammed Ahmed (1961) carried out regional geological mapping of the entire GSB and produced the first regional geological map. Sastry et. al., (1978) carried out detailed mineralogical mapping during in Hosur blocks and Ranganath and Jagannathan (1987) carried out preliminary exploration for gold in Hosur-Champion block of western GSB. A. G. Ugarkar and T.C. Devraj (1994) Ref. [5] has studied the auriferous zones of the GSB and are hosted by pillowed and sheared meta-volcanics in the western side and based on the relative

*Corresponding Author: Girish Kumar M.
Manuscript received May09, 2022; revised May 20, 2022.

doi: 10.18178/ijges.8.1.1-11

abundance of ore in the quartz veins and sulphide zones are classified into different types in the area.

Mining activity in selected areas of GSB was active since ancient to British period. The British companies developed some mines, processed about 48,700 tonnes of ore and recovered about 2,000 oz of gold during 1900 to 1911. Geological Survey of India systematically explored all the gold bearing tracts in the western half of the Gadag belt between Nagavi in the north and Sangli mines in the south, including Hosur and Yelisiruru. Bharat Gold Mines Ltd. (BGML) started a small experimental stopping and milling operation at Hosur-Champion mine which lasted for many years.

In the present paper aimed at augmenting the existing knowledge concerning ore fluid characteristics in meta-volcanic hosted gold deposits, in general and considering the western auriferous gold deposits as an example of Archean carton.

II. Geological Settings

The Dharwar Craton, especially the Western Dharwar Craton (WDC), hosts a number of N–S or NW–SE trending schist belts, such as Chitradurga, Gadag, Ajjanahalli and Shimoga, which occur within the Dharwar batholiths. The WDC is characterized by late Archaean volcanic and sedimentary rocks (Dharwar Supergroup; Swaminath *et al*, 1976) Ref. [6], that were deposited in the period of 2900-2600Ma (Balakrishnan et al, 1999; Vasudev *et al*, 2000) Ref. [7], [8]. The schist belts of Dharwar Supergroup are classified into two main divisions. The older, that is mainly igneous in character is named as the 'Bababudan Group' and hosts the main iron formations. The younger named as the Chitradurga group, which is more extensive group of schistose rocks and largely sedimentary in character, composed of conglomerate, quartzite, limestones, greywacke and associated manganiferous and ferruginous cherts.

The GSB, consists of both metavolcanic and metasedimentory rocks belonging to the Chitradurga Group of Archaean Dharwar Supergroup. The metavolcanics mainly consist of metabasalt, metabasaltic andesite, metaandesite, felsic rock (dacite, rhyolite) belonging to Ingaldhal formation and metasedimentaries consist of argillite, arenite, arkose, greywacke suite of rocks, banded iron formation and dolomite belonging to Hiriyur formations of Chitradurga Group. The western GSB consists of meta-volcanics i.e. meta-basalts, meta andesite and pyraxinites are occurs as lensoidal bodies and quartz veins are intruded in metabasalts. The central and eastern GSB consists of meta-volcaniccs of meta basalt and meta-sediments of greywacke, argillite and carbonate phyllites (Fig. 1). These rocks are strongly deformed, altered chloritised, carbonated and silicified.

Metabasalt occur both massive and schistose variety exhibits pillow structures and are well exposed in Hosur, Sortur, Varvi, Jalligere, Doni and Attikatti areas (Fig. 2). Both massive and schistose meta basalts are also exhibit pillowed character, vesicles occupy considerable portion of the rock, as seen near Mahalingeshwar Tanda and due to rapid cooling, the rocks show radical cracks. While some of the pillows are spherical and oval, most of them are deformed, showing elongation. Graded bedding is common in greywacke-argillite and is marked by gradation in grain size from coarse greywacke at the bottom to fine argillite/shale units at the top. Argillite suite of rocks also interbeded with BIF. Chlorite phyllite is seen around the central and eastern auriferous zones. Quartz-sericite phyllite is seen resting conformably on the chlorite phyllite. The quartz-serieite phyllite exposure west of Gouligeri Mutt (temple) lies along synclinal fold axis within the chlorite phyllite. A band of quartz-serieite phyllite of arcuate shape occurs in the amphibolite. The shale formations are enriched with silica and comprises of hematite, goethite and kaolinite in variable proportions. The bands of ferruginous/sulphidic chert occurring in the shale are usually thin but sometimes attain considerable thickness due to folding and are made up of alternating bands of hematite, magnetite and sulphidic chert.

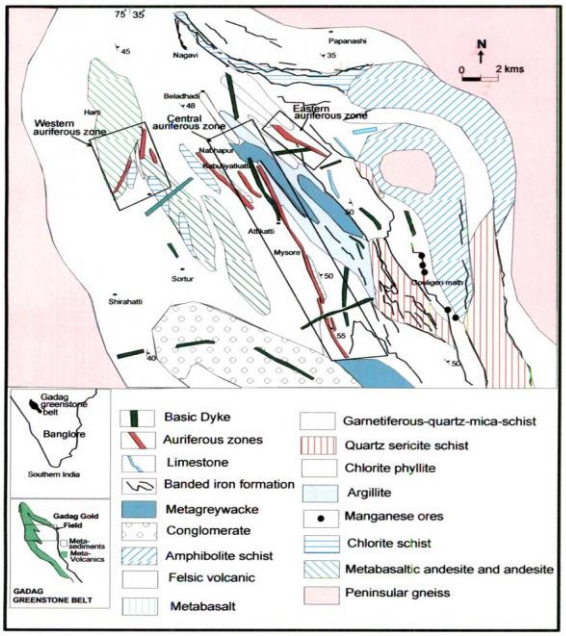

Figure 1. Geological map of Gadag Schist belt (modified after Ugarkar and Deshpande, 1999) Ref. [9].

Mineralised quartz veins are following NW-SE trend, which is the major foliation trend of the schistocity (S2) of the GSB (Fig. 3). Quartz veins (Milky-white series) were observed within metabasalt, meta-sediments and BIF and sulphide mineralised quartz veins are also intruded along the joint planes of the metabasalts Some quartz veins are gold mineralised and are mostly occur in the pillow metabasalt. The highly deformed nature of the pillows does not permit determination of the younging direction. Quartz veins are ubiquitous in the area and are emplaced along shear zones, faults and fractures. They are oriented along NNW-SSE, NW-SE and WNW-ESE directions. The quartz is milky white to smoky grey in color. Some of the quartz veins are associated with the shears controlling the auriferous lodes, as seen in (i) the volcanics hosted Hosur-Champion auriferous lodes, west of Shirunj (ii) argillites hosted Kabuliyatkatti-Attikatti-Mysore mine and Sangli mine auriferous lode system east

of Kabuliyatkatti and east of Mahalingeshwar Tanda and (iii) BIF hosted auriferous lode system north of Nagavi.

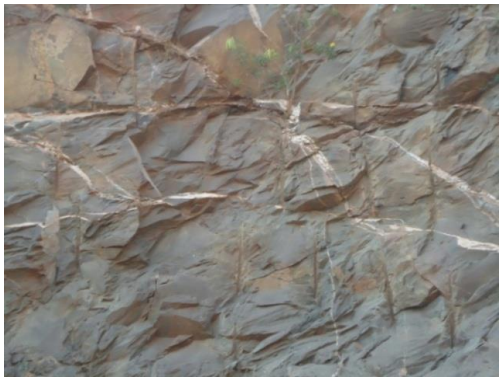

Figure 2. Metabasalt quarry at Harti village.

Figure 3. Mineralised quartz vein within the BIF

III. Gold Mineralisation

The metabasalts/pillowed metabasalt hosts gold mineralization. The pillowed metabasalt, carbonate and andesite are the marker horizon for gold mineralization in the western auriferous zone. Gold mineralisation occurs in quartz veins as well as associated with wall rock alteration (carbonitisation, chloritisation and seritisation). In addition, gold occurs both as free milling native metal and enclosed within sulphides, especially with pyrites. The en-echelon shear planes/ fractures and schistosity planes and sheared metavolcanic and metasediments are weak zones, which are impregnated by gold bearing quartz veins. Occasionally, minute discrete grains of gold are seen within the vein quartz. These features indicate that the shear zones hosting auriferous zone are ductile type. The ore minerals are native gold, arsenopyrite, pyrite, chalcopyrite, galena and scheelite.

IV. Ore Petrography

The native gold (free milling gold) occurs as irregular masses, stringers, droplets and along the micro fracture fillings. The gold associated with the sulphides especially with pyrite and arsenopyrite and along grain boundaries or within the pyrite. Pyrite occurs as cubic shape with slightly corroded margins and as aggregates. It shows yellowish white reflectance. It occurs as euhedral crystals and share mutual boundary with pyrrhotite and arsenopyrite crystal (Fig. 4a). Arsenopyrite is an iron arsenic sulfide (FeAsS) and occurs as fine to coarse grained, euhedral to subhedral crystals and as fracture fillings along with pyrrhotite (Fig. 4b). Chalcopyrite shows a golden yellowish in colour and it occurs in the fractures fillings. Chalcopyrite shows brass yellow colour and occurs as blebs and growth crystals in arsenopyrite.

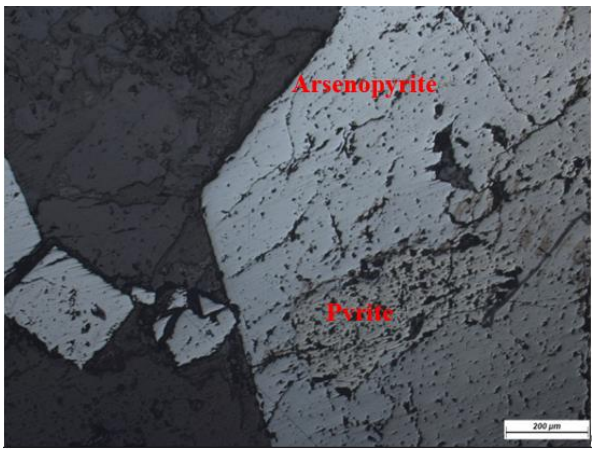

Figure 4a. Arsenopyrite crystals and pyrite within the Arsenopyrite.

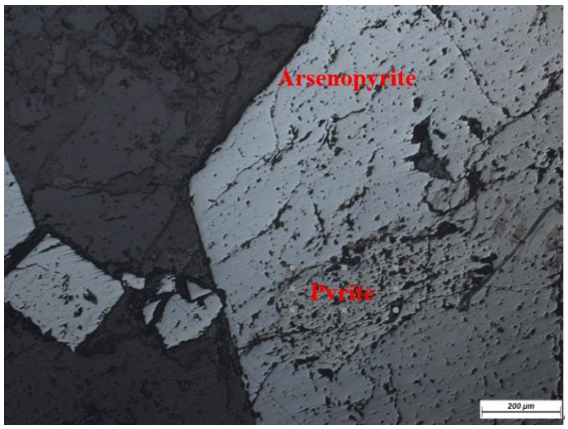

Figure 4b. Arsenopyrite crystals with Pyrrhotite

V. Analytical Techniques

To generate the analytical data, different analytical techniques were judiciously used by analyzing these samples along with international standards as mentioned in GSI's SOPs. Major oxides and trace elements of whole rock samples were determined using WD-XRF equipment (M/s. Bruker S8 Tiger) at NCEGR, RSAS, GSI, Bengaluru. For the REE analysis the samples were powdered to -200 # manually in an agate mortar after preparing rock granules in a hand operated steel mortar. the analysis were carried out by LA-ICPMS (Perkin Elmer SCIEX ELAN DRC-II) at Chemical division, GSI, Southern Region, Hyderabad using international standards JB-2 and BHVO-1, following routine analytical protocol given by Balram *et, al*. (1996) Ref. [10].

The fresh samples were collected from the field preparation of thin sections, polish sections and wafers for petrography, EPMA and fluid inclusion studies. Mineral phases of sulphide, silicate and oxides were analysed using a CAMECA SX-100 Electron Microprobe Analyser

(EPMA) equipped with five wavelength dispersive spectrometers (WDS) at NCEGR, GSI, Bangalore. Calibration, overlap correction and quantifications were performed with the CAMECA SX- 100 Peak Sight-Geo Quanta software package. Sulphide and nobel metal phases were analysed using 20 kV acceleration voltage and 20 nA beam current with beam 1 µm size.

Images of fluid inclusions from wafers of quartz veins were displayed on a monitor for observation, using Olympus BX51 microscope manufactured by Fluid Inc. (USA), and a high-resolution camera. Based on their petrographic character, various fluid inclusions in the mineralized quartz veins were selected for microthermometric measurements. The fluid inclusions were analyzed with LINKAM MDSG-600 heating-freezing stage, fitted on Olympus BX-51 petrological microscope housed in NCEGR, GSI, Bangalore. The unit operates in the temperature range of -195 to 600 ºC, and is periodically calibrated by synthetic pure H_2O inclusions (0 ºC) and H_2O-CO_2 inclusions (-56.6 ºC). The accuracy of the measured temperatures is about ±0.2 ºC during cooling and about ±2 ºC between 100 and 600 ºC. The salinities of NaCl-H_2O inclusions were calculated using the final melting temperatures of ice (Bodnar, 1993). The salinities of three-phase NaCl-CO_2-H_2O fluid inclusions were calculated using the melting temperatures of clatharate (Collins, 1979) Ref. [11]. Calculations of fluid density, salinity and construction of isochores were done using PVTX (version 2.0) software of M/s. Likam, UK. Subsequently FLUIDS 2003 package (Bakker, 2003) Ref. [12]. (AQSO, BULK, Q2 and ISCO programs were utilized. FLUIDS soft- ware incorporates the equations of state (EOS) of Thiery *et al.* (1994) Ref. [13], Duan *et al.* (1992) Ref. [14]. for CO_2±CH_4 system (carbonic inclusions) and those of Archer (1992) Ref. [15] and Zhang and Frantz (1987) Ref. [16] for H_2O-NaCl system (aqueous inclusion) and H_2O- NaCl-CO_2(V)-CO_2(L)±CH_4 (aqueous carbonic inclusions).

A. Geochemical Analysis

The whole rock geochemistry (Table I) of the major litho unit of metabasalt reveals that the SiO_2 content is varying from 37.96 to 49.38, Al_2O_3 from 10.12 to 16.65 and FeO (T) from 12.84 to 22.17. Interestingly the MgO (4.66 to 11.78), CaO (2.94 to 11.04) and K_2O (0.10 to 2.94) content are very high due to the presence of neominerals like chlorite, sericite and carbonates, which were developed during the hydrothermal alterations of the host metabasalt. The A/NK vs A/CNK plot indicates the metaaluminous composition (Fig. 5a). The ore zone quartz vein samples shows higher content of CaO, due to the presence of fragments of carbonates in the wall rocks of the veins and theses carbonates were developed during the hydrothermal activity.

The REE Geochemistry of host metabasalt is varying from 39.75 to 150.89 ppm (average 69.17) and the ΣLREE varies from 23.47 to 103.90 and ΣHREE varies from 7.45 to 44.47 (Table II). The REE exhibit very slightly enriched LREE (Ce/Yb = 6.67) to flat pattern of HREE, without any Eu anomaly (Fig. 5b). The ore zone shows ΣREE (40.53 to 233.45 ppm) (Table III) and the pattern reveals enriched in LREE (Ce/Yb = 23.41) and HREE depleted and flattened without any Eu anomaly (Fig. 5c). These samples were become more fractionated with the abundance of LREE increasing to a greater extent with depletion of HREE. Thus wall rock alteration zone involves significant addition of LREE from the host rock metabasalt without any addition to HREE. These enrichment of LREE relates with respect to increasing degree of wall rock alteration and the REE pattern of ore zone quartz vein shows low abundance as these are hydrothermal quartz veins.

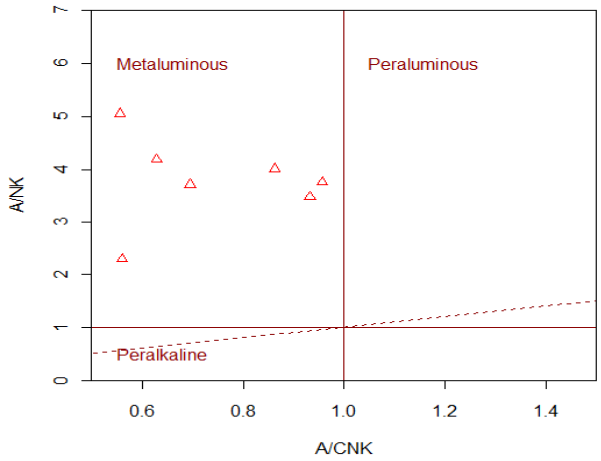

Figure 5a. A/NK vs A/CNK plot (Shand, 1943)

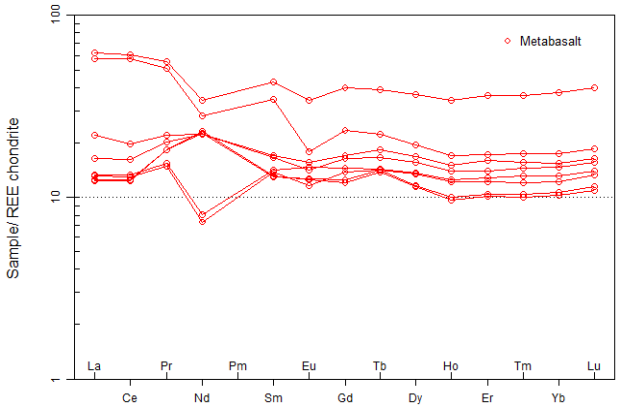

Figure 5b. Chondrite-normalized REE diagrams (Boynton, 1984)

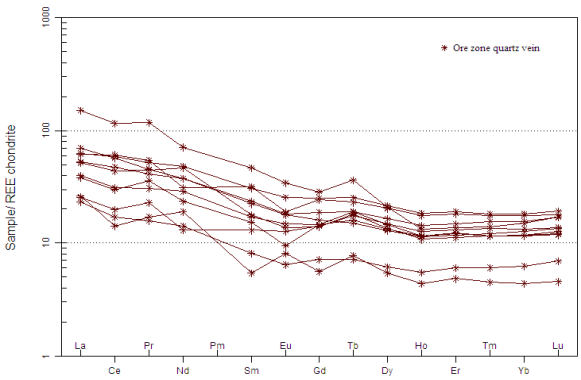

Figure 5c. Chondrite-normalized REE diagrams (Boynton, 1984)

B. Mineral Chemistry

Microprobe analyses of each mineral in the mineralized quartz veins were carried out along with capturing of BSE images. Special emphasis was laid in analyzing gold and sulphides and other ore minerals. EPMA and EDX studies were carried out for the ore minerals of gold and sulphides. The gold grains are euhedral in shape and size varies from 3 to 6 µm and found within the pyrite grains and is confirmed from EPMA studies and the arsenopyrite grain shows euhedral with sharp edges (Fig. 6a, b), the EDX images of the analysis are given below. The EPMA analysis of samples from western auriferous zone of GSB Gold grain analysis data is given below (Table IV).

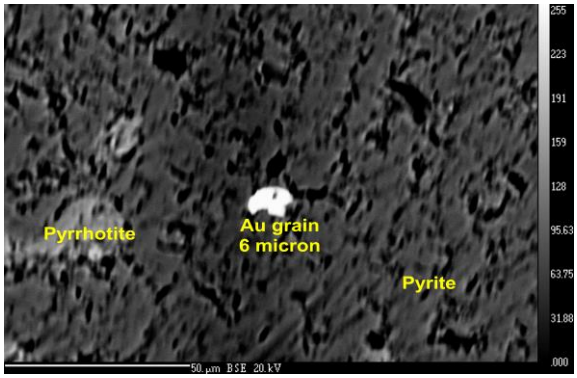

Fig. 6a BSE images showing gold grain associated with pyrite.

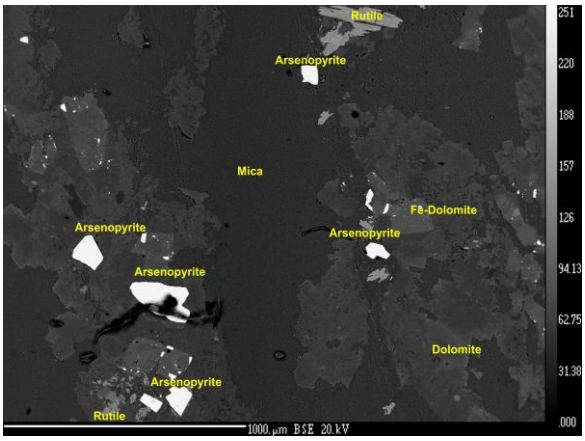

Figure 6b. BSE images showing arsenopyrite.

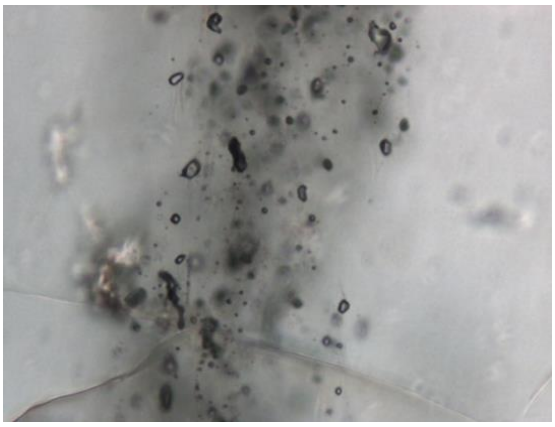

Figure 7a carbonic inclusions.

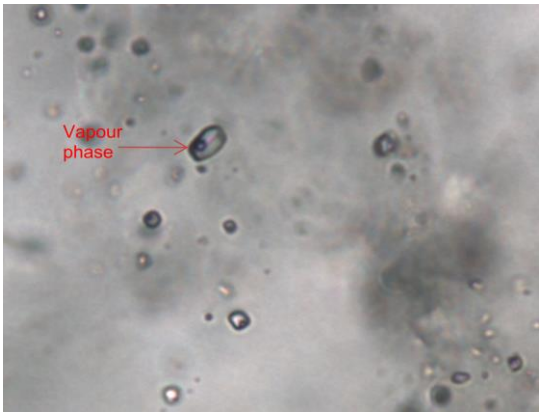

Figure 7b. Aqueous inclusions.

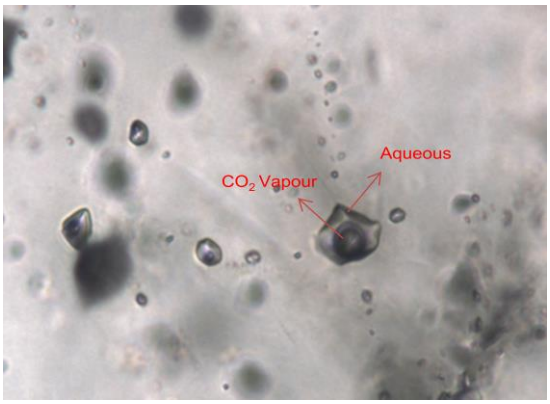

Figure 7c. Aqueous carbonic inclusions.

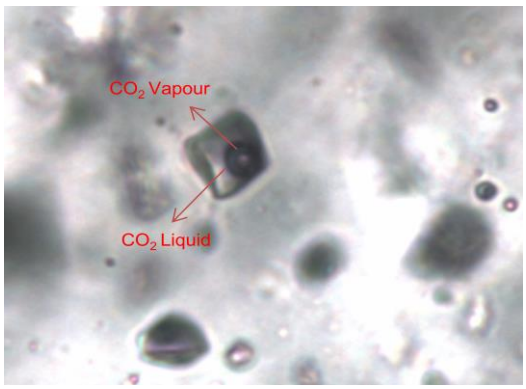

Fig. 7d. Aqueous carbonic inclusions

C. Fluid Inclusion Studies

Fluid inclusion parameters of the auriferous zones samples were studied and the identification of inclusions were based on genetic nature and mineral phases. A large number of fluid inclusions, including primary, pseudo secondary and secondary fluid inclusions were identified using detailed petrographic observations. In accordance with the classification principles and techniques outlined by Roedder (1984) [17]. An attempt was made in the light of new experimental studies by Bodnar, R. J. et al. (1989) [18], on the morphology of fluid inclusions to correlate the different textural features of fluid inclusions. Oriented samples of mineralized quartz veins from trenches/abandoned mines were collected for the detailed studies of nature and composition of trapped fluids which were responsible for mineralization in the area.

The fluid inclusion present within the individual quartz grains occur as isolated, cluster and some are intragranular and also along the grain boundaries. Based on the phases present in the inclusions are monophase, liquid rich and vapour rich biphase at room temperature. The monophase fluid inclusions are common and are dominantly contain CO_2 phase. The liquid rich biphase inclusions abundant and contain vapour of H_2O with liquid H_2O. The vapour rich biphase inclusions are rare and mostly contain CO_2 which is surrounded by liquid H_2O and contain carbonic phases. The intra-granular and trans-granular trails are generally observed and contain extremely small and highly distorted monophase and biphase inclusions.

They are grouped into three types: type-I primary monophase carbonic inclusions, type-II primary aqueous carbonic inclusions and type-III primary aqueous bi-phase inclusions. Type-I inclusions are common and these inclusions contain only one phase. The CO_2 vapour is perfectly circular and spherical (Fig. 7a) and few of the CO_2 vapour bubble shows a dark rim in the periphery at room temperature which is due to the presence of a thin film of liquid CO_2 over vapour CO_2 and are homogenized into the liquid phase. The type-II inclusions are less abundant and not so common, these inclusions occur in isolated pattern and contain CO_2 (liquid)+CO_2 (gas)+H_2O(liquid)+NaCl (Fig. 7b). The aqueous carbonic inclusions often show varying degrees of fill. The type-III inclusions are comparatively more abundant than any other inclusions and these inclusions occur as isolated and clustered (Fig. 7c & d). They are generally small and rounded as well as irregular and contain two phases, liquid (H2O+NaCl) and a vapour bubble H2O (vapour), that is homogenized to liquid upon heating.

D. Microthermetric

Microthermometric measurements of fluid inclusions in mineralized quartz veins from western, central and eastern zones are summarized in Table V.

The type-I inclusions are primary carbonic inclusions formed solid CO_2 upon cooling. The solid CO_2 melt at the temperature between -56.6ºC and -62ºC. In most of the inclusions and in few inclusions the melting temperature observed at lower temperature is -58.5ºC, 59.0 ºC, -59.3 ºC and 61.5ºC. This lowering of melting temperature of CO_2 indicating admixtures of other gases such as N_2 & CH_4 (Brown and Lamb, 1989) [19]. The temperature of homogenized of CO_2 into vapour phase at temperature 11.2 to 28.0 ºC (density varies 0.65 to 0.85 g/cm3).

The primary aqueous carbonic inclusions (Type-II), which are comparatively less abundant and not so common like the aqueous inclusions, occur as isolated and also cluster type patterns. These inclusions are characterized by the nucleation of a vapour bubble on cooling, consistent with the composition, CO_2(liquid)+CO_2(gas)+H_2O(liquid)+NaCl. These aqueous carbonic inclusions often show varying degrees of fill and coexist with aqueous rich inclusions, suggesting that the fluid immiscibility might have occurred towards the stage of crystallization (Roedder, 1984). The range of homogenization temperature varies from 212ºC to 290ºC. The eutectic temperatures (*T*e) range from -15ºC to -25ºC with an average of -20.45ºC and this suggests that the major component in aqueous phase is ±KCl with NaCl in the fluid system. The final melting temperature of ice (Tm_{ice}) ranges from -0.5ºC to -5.2ºC corresponding with salinities of 0.82 wt.% to 8.09 wt.% NaCl eq. following the equations of Bodnar (1993) [20]. The melting temperature of CO_2 of the aqueous carbonic inclusions ranges from -56.7°C to -57.2°C and the homogenization temperature ranges from 15.0 to 30.0°C. The CO_2 density of carbonic aqueous varies from 0.74 to 0.89 g/cm^3 with an average of 0.80 g/cm^3.

TABLE I. GEOCHEMICAL DATA OF THE METABASALT ROCK (MAJOR OXIDES AND TRACE ELEMENTS)

	GA-W-01	GA-W-02	GA-W-06	GA-W-07	GA-W-12	G-W-101	G-W-103A	G-W-106	G-W-107
SiO2	44.06	42.01	44.2	49.38	37.97	38.24	44.63	43.5	37.96
TiO2	1.84	0.95	0.57	0.62	0.45	0.54	0.85	1.03	0.58
Al2O3	10.12	10.81	11.52	14.92	13.32	13.85	13.04	12.84	16.65
Fe2O3	21.85	16.77	15.7	12.84	20.06	22.17	14.94	18.19	14.16
MnO	0.23	0.24	0.21	0.13	0.19	0.13	0.17	0.19	0.17
MgO	2.94	7.7	11.04	3.72	3.17	4.45	6.31	8.23	6.88
CaO	7.5	11.78	10.14	6.4	9.89	4.66	8.39	5.56	8.34
Na2O	2.4	1.7	1.32	0.48	0.56	0.26	2.01	2.16	1.88
K2O	0.43	0.1	0.1	2.94	2.09	1.98	0.19	0.12	0.98
P2O5	0.33	0.1	0.09	0.14	0.1	0.11	0.07	0.09	0.06
LOI	8.3	7.84	5.11	8.43	12.2	13.61	10.2	6	13.03
Total	91.7	92.16	94.89	91.57	87.8	86.39	100.8	97.71	100.69
Sc	39	52	30	26	40	34	47	47	42
V	158	298	193	143	176	221	262	319	248

Cr	52	256	302	155	207	188	248	283	249
Co	39	39	48	9	24	66	65	64	43
Ni	11	113	218	72	100	132	96	111	94
Cu	172	134	194	317	183	519	82	84	85
Zn	139	137	126	274	1390	469	88	109	82
Ga	16	15	9	11	17	17	14	17	14
Rb	5	5	5	77	46	57	5	8	23
Sr	92	117	79	44	58	27	75	88	74
Y	50	22	19	22	24	19	18	21	15
Zr	132	71	57	183	145	91	66	72	69
Nb	10	6	7	15	8	9	10	11	11
Ba	147	50	50	442	260	142	<50	90	51
Pb	8	13	12	5	4	7	6	6	5
Th	7	4	5	11	14	13	<5	<5	<5

TABLE II. REE OF METABASALT ROCK

	GA-W-01	GA-W-02	GA-W-06	GA-W-07	GA-W-12	G-W-101	G-W-103A	G-W-106	G-W-107
La	6.79	3.86	5.11	9.53	3.81	19.27	4.11	4.06	17.92
Ce	15.85	10.09	13.12	14.82	9.94	48.92	10.73	10.54	46.86
Pr	2.69	2.25	2.46	3.54	2.24	6.82	1.88	1.82	6.22
Nd	13.37	13.57	13.33	22.12	13.84	20.45	4.86	4.36	16.94
Sm	3.25	2.52	3.30	1.44	2.58	8.45	2.77	2.69	6.76
Eu	1.05	0.93	1.15	0.49	0.92	2.52	1.08	0.86	1.32
Gd	4.23	3.23	4.40	1.88	3.14	10.40	3.76	3.58	6.05
Tb	0.79	0.67	0.87	0.62	0.65	1.86	0.68	0.67	1.06
Dy	5.01	3.77	5.40	2.29	3.69	11.82	4.41	4.33	6.30
Ho	1.00	0.72	1.08	0.33	0.70	2.44	0.90	0.88	1.21
Er	2.94	2.18	3.36	0.98	2.14	7.59	2.69	2.56	3.60
Tm	0.47	0.34	0.50	0.16	0.33	1.18	0.43	0.39	0.57
Yb	3.06	2.22	3.20	1.02	2.16	7.88	2.76	2.57	3.63
Lu	0.50	0.37	0.53	0.17	0.35	1.29	0.45	0.43	0.60
ΣREE	60.98	46.72	57.82	59.38	46.50	150.89	41.49	39.75	119.02
LREE	41.94	32.29	37.33	51.44	32.42	103.90	24.24	23.47	94.70
HREE	17.99	13.50	19.35	7.45	13.17	44.47	16.06	15.41	23.01
LREE/HREE	2.33	2.39	1.93	6.90	2.46	2.34	1.51	1.52	4.12
CeN/YbN	5.18	4.54	4.09	14.49	4.61	6.21	3.89	4.10	12.92

TABLE III. REE OF OREZONE

Orezone	GA-W-08	GA-C-13	GA-C-21	GA-C-23	GA-C-24	GA-E-33	GA-E-34	G-W-103C	G-W-103H	G-W-107	W-G-225
La	8.03	21.72	12.40	7.78	16.15	16.50	19.57	46.84	7.16	19.00	11.92
Ce	11.38	46.32	25.21	15.88	35.54	38.51	47.66	93.91	13.68	49.46	24.28
Pr	2.07	5.53	3.76	2.77	5.47	5.08	6.40	14.41	1.92	6.69	4.41
Nd	11.32	22.72	17.37	7.80	28.15	22.74	28.99	42.83	8.43	18.75	13.94
Sm	1.05	4.32	3.31	2.52	3.43	4.52	6.04	9.15	1.58	6.22	2.97
Eu	0.59	1.30	1.08	0.93	1.00	1.33	1.86	2.53	0.47	1.38	0.70
Gd	1.45	4.10	3.74	3.65	3.61	4.83	6.46	7.40	1.84	6.22	3.74
Tb	0.37	0.71	0.76	0.83	0.86	0.90	1.19	1.72	0.34	1.08	0.89
Dy	1.74	4.15	4.25	4.73	4.33	5.25	6.87	6.66	1.97	6.51	4.67
Ho	0.31	0.81	0.82	0.91	0.77	1.02	1.31	0.95	0.39	1.25	0.83

Er	1.01	2.45	2.54	2.72	2.34	3.08	3.95	2.84	1.26	3.79	2.57
Tm	0.15	0.39	0.38	0.43	0.37	0.50	0.58	0.45	0.20	0.56	0.37
Yb	0.92	2.63	2.42	2.77	2.43	3.23	3.78	3.12	1.30	3.67	2.43
Lu	0.15	0.43	0.38	0.44	0.39	0.55	0.61	0.54	0.22	0.57	0.41
ΣREE	40.54	117.58	78.41	54.18	104.84	108.04	135.28	233.35	40.77	125.16	74.14
LREE	33.86	100.61	62.06	36.74	88.75	87.35	108.66	207.13	32.78	100.12	57.53
HREE	6.09	15.67	15.27	16.50	15.09	19.35	24.76	23.69	7.52	23.66	15.91
LREE/HREE	5.56	6.42	4.06	2.23	5.88	4.51	4.39	8.74	4.36	4.23	3.62
CeN/YbN	12.43	17.62	10.43	5.73	14.65	11.91	12.60	30.10	10.51	13.47	10.00

TABLE IV. GOLD GRAIN ANALYSIS DATA BY EPMA

Weight%										remarks
S	Fe	Co	Cu	Zn	As	Pb	Ni	Ag	Au	Total	
1.58	20.84	0	0	0	0	0	0	9.74	84.64	98.8	Gold
5.98	5.57	0	0.07	0	0	0	0	9.46	82.32	103.41	Gold
2.66	3.79	0	0	0	0	0	0.03	9.8	84.22	100.5	Gold
3.21	4.2	0.02	0	0	0	0	0.01	9.33	83.45	100.23	Gold
2.4	5.07	0	0.09	0	0	0	0	4.84	82.64	95.05	Gold
9.24	8.38	0.03	0.06	0	0.03	0	0.07	4.74	83.00	105.55	Gold

TABLE V. PRIMARY FLUID INCLUSION DATA OF THE MINERALISED QUARTZ VEIN

Mineralized Quartz vein	**FI type**	**N**	**Tm_{Co2} (ºC)**	**Th_{Co2} (ºC)**	**Te (ºC)**	**Tm_{ice} (ºC)**	**Th total (ºC)**	**Tm clath (ºC)**	**Salinity (wt. % NaCl eq.)**	**Density g/cm^3**
Western zone Mineralized Quartz vein	Type-I	52	-56.6 to -62.0	11.2 to 28						0.65 to 0.85
	Type-II	32	-56.6 to -57.2	24 to 30	-16 to -24	-1.2 to -5.2	212 to 286	8.1 to 10.2	1.97 to 8.09	0.75 to 0.89
	Type-III	72			-15 to -25	-0.5 to -5.0	180 to 245		0 .83 to 7.81	0.84 to 0.94
Central zone Mineralized Quartz vein	Type-I	56	-56.6 to -58.2	13.1 to 28						0.65 to 0.83
	Type-II	39	-56.6 to -57.2	15 to 29	-15 to -25	-0.5 to -3.8	220 to 290	9.5 to 11.0	0.82 to 6.07	0.74 to 0.85
	Type-III	85			-15 to 23	-0.5 to -3.8	162 to 242		0 .82 to 6.07	0.85 to 0.93
Eastern zone Mineralized Quartz vein	Type-II	39	-56.8 to -57.1	25 to 29	-15 to -24	-1.0 to -3.8	220 to 250		1.65 to 6.07	0.74 to 0.85
	Type-III	85			-20 to -29	-2.4 to -5.8	167 to 192		3.91 to 8.91	0.90 to 0.95

The type-III inclusions are aqueous inclusions and are frozen at temperatures mainly between -58ºC to -79ºC. The range of homogenization temperature varies from 160ºC to 245ºC and during the heating runs the first melting (eutectic) temperature (*Te*) has been observed, ranging from -15 to -29 ºC with an average of -20.70ºC and suggesting that the major component in aqueous phase is ±KCl with NaCl in the fluid system. The maximum eutectic temperature -29 ºC may indicate the presence of NaCl±KCl±$MgCl_2$ and H_2O (Shepherd *et al.*, 1985) [21]. The final melting temperature of ice (*T*m, ice) ranges from -0.5 to -5.8ºC (average -2.88ºC) corresponding salinities of 0.82 to 8.91 wt.% NaCl eq. The density of aqueous varies from 0.84 to 0.95 g/cm^3.

VI. DISCUSSION AND CONCLUSION

The Gadag schist belt is the northern continuation of the eastern limb of well known CSB (Dharwar Type) of Archean age 2600 Ma years, which was explored since ancient times. The lithological association of the GSB includes metavolcanic (metabasalt to felsic volcanics) and metasedimentary rocks (conglomerate, greywacke, argillite, arenite, arkoses, phyllite, banded iron formation and limestone/dolomite)., which are surrounded by older TTG and younger granitoids. In GSB, three parallel and tabular auriferous zones, namely western, central and eastern auriferous zones that run in a linear pattern almost sub-parallel to regional foliation (i.e. NNW-SSE). i)Western zone comprising Hosur-Champion, Yelishirur and Venkatapur mines hosted dominantly in metabasalts and metaandesites (ii) Central zone comprising Kabulayatkatti-Attikatti, Mysore Mine and Sangli Mine, hosted mostly in greywacke. In addition, gold mineralisation is also known from the area north of Nagavi which are hosted in BIF and in contact with tuffaceous rocks (iii) Eastern zone comprising Sankatodak block and a fewer prospects of east of Nabhapur and Kabulayatkatti villages which are hosted in greywacke.

The western lode system comprises of Hosur-Champion Reef -Yelisirur areas. This zone is hosted by pillowed metabasaltic andesite and meta andesite and chlorite schist along the contact of quartz porphyry. A total of about 8 major and many minor lodes constitute the system which extends southwards for about 6.5 kms from north-east of Hosur village to south of Yelisirur and Venkatapur villages. The pillowed metabasalt and metaandesite are the marker horizon for gold mineralization and it is controlled by NNW-SSE trending shear zones. The central lode system is about 6 kms east of the western system and the mineralized zone occurs both in schistose metavolcanics and metasediments. The

mineralization is found within both medium grained thick bedded, massive beds and thin bedded sequence of graywackes-argillite-phyllite formations. The eastern lode is situated from north of Kabulayatkatti block and Sankatodak area. The lithology mainly consist of meta-graywacke-argillite, chlorite-phyllite and metaaranite. The mineralisation occurs in the vicinity of carbonaceous matter, brecciated veins in carbonaceous rocks, quartz and chert association. The gold mineralisation in the GSB mainly confined to the white and smoky quartz veins of varying width along shear exhibits evidences of strong alterations characterised by chloritsation, sericitisation, carbonatisation and silicification and also associated with sulphides like pyrite (most abundant sulphide mineral) pyrrhotite, arsenopyrite and chalcopyrite.

A. Geochemistry and REE Analysis

The whole rock geochemistry of metabasalt reveals that the MgO (4.66 to 11.78), CaO (2.94 to 11.04) and K_2O (0.10 to 2.94) content are very high due the presence of minerals like chlorite, sericite and carbonates were developed during the hydrothermal alterations of the host metabasalt. The A/NK vs A/CNK plot indicates the peraluminous composition. The ore zone quartz vein samples shows higher content of CaO are due to the presence of fragments of carbonates in the wall rocks of the veins and theses carbonates were developed during the hydrothermal activity.

The REE geochemistry of host metabasalt is varies from 39.75 to 150.89 ppm (average 69.17). The samples become more fractionated with the abundance of LREE increasing to a greater extent, with slight depletion of HREE. The REE pattern of ore zone quartz vein (40.54 to 233.35) shows low abundance because these quartz veins are of hydrothermal quartz veins.

The REE patterns of the wall rock alteration zone and ore zone quartz veins reveals that the enriched LREE and depleted HREE due to the activity of hydrothermal fluids responsible for alteration of wall rocks and precipitation of ore zone quartz vein (carbonates, sulphides and gold) and the REE content has derived, most probably from the host rocks (metabasalt rock).

B. EPMA Analysis

The mineralised quartz veins were studied by EPMA and found the gold grains of about 3 to 6 micron within the pyrite grain and other sulphides namely arsenopyrite, chalcopyrite and pyrrhotite. The analysis of the gold grain reveals that the Au contain 84.64 to 82.64 wt. % and Ag contain 4.84 to 9.74 wt. %.

C. Fluid Inclusions Studies

Fluid inclusion studies were carried out in the auriferous zones of western, central and eastern zones of the GSB. The western and central zone reveals three types of fluid inclusions i.e type-I are monophase carbonic inclusions, type-II are aqueous inclusions and type-III are aqueous carbonic inclusions and eastern zone shows two types (type-II & type-III). The total homogenisation temperature (Th_{total}) of the western and central zone varies from 180 to 286°C and 162 to 290°C. The salinity of western and central varies from 0.83 to 8.09 wt.% NaCl equivalent and 0.82 to 6.07 wt.% NaCl equivalent. The eastern zone shows slightly decreased the total homogenisation temperature (Th_{total}) i.e. 167 to 250°C and the salinity (1.32 to 8.91 wt.% NaCl equivalent) are in the same ranges as compare to the western and central zones. The aqueous carbonic inclusions (type-III) are showing higher total homogenisation temperature (Th_{total}) of about maximum 290°C, which represent the exact trapping temperature, because of the occurrence of the phase separation (Roeder, 1984). Phase separation in aqueous carbonic inclusion (H2O+CO2+NaCl) fluid system is a mechanism, which cause gold deposition in a variety of environments and fluid inclusion studies have demonstrated the existence of low saline, immiscible CO_2 and H_2O rich fluids relates to ore in a number of gold deposit (Mishra and Panigrahi, 1991) [22]. The CO_2 seems to be an almost universal constituent of the ore fluids depositing gold and it forms major constituents of most of fluid inclusions in gold ores from the metamorphic environment. Hutchison (1993) [23] that in such environment gold might have been carried as carbonyal or carbonate complex and that the extraction of CO_2 from the ore fluids by reaction with divalent cations in the wall rock to form carbonates, would result in the precipitation of gold within suitable structural sites (shear zone) through a combination of decreasing temperature and fluid-wall rock interaction, progressive carbonization of wall rocks with decreasing temperature and pressure might lead to fluid immiscibility and separate H2O-rich and CO2 rich phases. These physical separations of two immiscible fluids significantly change the solubility of gold and thus cause precipitation (Groves and Foster, 1993) [24] in the form of quartz veins.

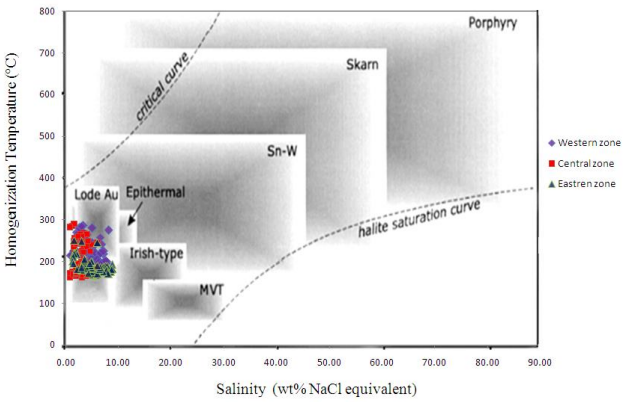

Figure 8. Homogenization temperature vs Salinity diagram illustring typical ranges for inclusions from differenct deposist types (Wilkinson, 2001).

The initial ice melting temperatures (T_{FM}) range from -25°C to -15°C with an average of – 21.25 °C, suggests that the major component in aqueous phase is ± KCl with NaCl in the fluid system. The maximum of first ice melting temperature of -25°C may indicate the presence of NaCl ± KCl with H_2O (Shepered, Rankin and Aldertron, 1985). The final melting temperature of ice ranges from -1.2°C to -5.2°C (average -2.4°C) corresponding with salinities of 1.97 to 8.09 wt.% NaCl equivalent (average

3.75 wt.% NaCl equivalent). The carbonic inclusions shows depression in $Tmco_2$ (ranges from -62.2°C to -56.6°C) due to the presence of traces of CH_4 with CO_2 which is also confirmed by Raman spectroscopy.

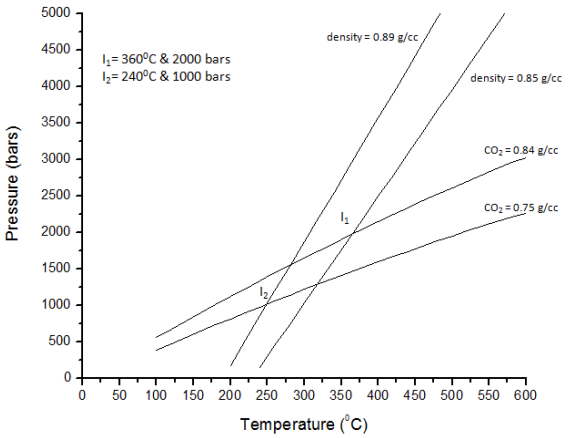

Figure 9. Isochors of PT condition of the fluid inclusion analysis of densities of each inclusion types.

The Salinity vs total homogenisation temperature (Th_{total}) diagram illustrating typical ranges for inclusions from different types (Wilkinson. J. J. 2001) [25], All three zone of GSB fall in the lode Au (gold) deposits (Fig. 8). The deduced gross fluid composition, salinity and P-T condition of the study area are comparable with the published data from other gold and sulphides in the Archean hydrothermal deposits in the granite-greenstone belts shows 250 to 400°C and salinity 2 to 6 wt% NaCl equivalent (Brown and Lamb, 1986; Groves, 1993).

The P-T condition was estimated using the FLUIDS package (Bakker, 2003). The estimated the P-T condition ranging from 220 to 375°C and 0.9 to 2.0 K bar, which almost matches with the other lode gold deposits PT condition of the Archean Dharwar craton (Fig. 9).

Further, the auriferous zones of GSB are structurally controlled and low salinity sulphur carbonate rich hydrothermal fluid of moderate temperature range and intense wall rock alteration (silicification, carbonatization and chloritsation) during the fluid –wall rock interaction within the suitable site (shear zone) below Amphibloite – greenschist facies transition. The Ore fluids of the GSB with other gold deposits in the Dharwar Craton, confirms that fluids of low saline and aqueous–carbonic composition with metamorphic parentage played the most dominant role in the formation of the Archean lode gold systems.

Conflict of Interest

The authors declare no conflict of interest.

Acknowledgment

The authors would like to express their gratitude and sincere thanks to Dr. S. Raju, Director General, Geological Survey of India and Shri Debkumar Bhattacharya, Deputy Director General & HOD, RSAS, Geological Survey of India, Bangalore for constant guidance. A special thanks to Dr. D. S. Jeere and Smt. Gargi Bhattacharya, Director's, RSAS Geological Survey of India, Bangalore for reviewing and giving valuable suggestions to improve the manuscript. In addition, sincere thanks to officials of NCEGR and RSAS for their continuous guidance and support, motivation and encouragement to carry out this work.

References

[1] J. R. Ridley and L. W. Diamond, "Fluid chemistry of orogenic lode gold deposits and implications for genetic models," *Reviews in Economic Geology*, vol. 13, pp. 141-162. Jan 2000.

[2] R. Kerrich, "Mesothermal gold deposits: A critique of genetic hypothesis," *Greenstone Gold and Crustal Evolution, NUNA conference Volume*, Geological Association of Canada, St Johns, Newfoundland, 13-31, 1991.

[3] D. I. Groves, R. J. Goldfarb, F. Robert, and C. J. R. Hart, "Gold deposits in metamorphic belts: Overview of current understanding, outstanding problems, future research, and exploration significance," *Economic Geology*, vol. l, pp. 1-29, 2003.

[4] J. Kolb, A. Rogers, and F. M. Meyer, "Relative timing of deformation and two-stage gold mineralization at the Hutti Mine," *Dharwar Craton, India. Mineralium Deposita*, vol. 40, pp. 156 to174, 2005.

[5] A. G. Ugarkar and T. C. Devaraju, "Ore mineralogy of Western Auriferous zone of gadag greenstone belt, Karnataka," *Journal of the Geological Society of India*, vol. 43, pp. 549–555, 1994.

[6] J. S. Nath, M. Ramakrishnan, and M. N. Viswanatha, "Dharwar stratigraphic model and Karnataka craton evolution," *Records of the Geological Survey of India*, vol. 107, 149–175, 1976.

[7] S. Balakrishnan, G. N. Hanson, and V. Rajamani, "Pb and Nd isotope constraints on the origin of high Mg and tholeiitic amphibolites, kolar schist belt, South India," C*ontributions to Mineralogy and Petrology*, vol. 107, pp. 279-292, 1990.

[8] V. N. Vasudev, B. Chadwick, A. P. Nutman, and G. V. Hegde, "Rapid development of late Archean Hutti schist belt, northern Karnataka: Implications of new field data and SHRIMP zircon ages," *Journal of the Geological Society of India*, vol. 55, pp. 529-540, 2000.

[9] A. G. Ugarkar and M. P. Deshpande, "Lithology and gold mineralization of gadag gold field, dharwar craton — Evidences for epigenesis of gold in diversified host rocks," I*ndian Mineralogist*, vol. 33, pp. 37–52, 1999.

[10] S. Balakrishnan, G. N. Hanson, and V. P. Rajamani, "Nd isotope constraints on the origin of high Mg and tholeiitic amphibolites," *Kolar Schist Belt, South India, Contributions to Mineralogy and Petrology*, vol. 107, pp. 279 – 292, 1990.

[11] P. L. F. Collins, "Gas hydrates in CO2-bearing fluid inclusions and the use of freezing data for estimation of salinity," *Economic Geology*, vol. 74, no. 6, pp. 1435–1444, 1979.

[12] R. J. Bakker, "Package fluids, computer programs for analysis of fluid inclusion data and modeling bulk fluid properties," *Chem. Geol.*, vol. 194, pp. 3–23, 2003.

[13] R. Thiéry, J. Videl, and J. Dubessy, "Phase equilibria modeling applied to fluid inclusions, liquid–vapor equilibria and calculation of the molar volume in the CO_2–CH_4–N_2 system," *Geochimica et Cosmochimica Acta*, vol. 58, pp. 1073–1082, 1994.

[14] Z. Duan, N. Møller, and J. H. Weare, "An equation of state for the CH_4–CO_2–H_2O system: II. Mixtures from 50 to 1000 °C and 0 to 1000 bar," *Geochimica Et Cosmochimica Acta*, vol. 56, pp. 2619–2631, 1992.

[15] D. G. Archer, "Thermodynamic properties of the NaCl–H_2O system: II. Thermodynamic properties of NaCl(aq), NaCl. $2H_2O$(cr), and phase equilibria," *Journal Physical Chemistry Reference Data*, vol. 21, pp. 793–829, 1992.

[16] Y. G. Zhang and J. D. Frantz, "Determination of the homogenisation temperatures and densities of superficial fluids in the system NaCl-KCl-$CaCl_2$-H2O using synthetic fluids inclusions," *Chem. Geol*., vol. 64, pp. 335-345, 1987.

[17] E. Roeder, "Fluid inclusions," *Reviews in Mineralogy*, vol. 12, 1984

[18] R. J. Bodnar, P. R. Binns, and D. L. Hall, "Synthetic fluid inclusions-vi, quantitative evolution of the decrepitation behavior of fluid inclusions in quartz at one atmosphere confining pressure," *Jour. Met. Geol*., vol. 7 pp. 229-242, 1989.
[19] P. E. Brown and W. M. Lamb, "P-V-T properties of fluids in the system H_2O-CO_2-NaCl: New graphical presentation and implications for fluid inclusion studies," *Geochim. Cosmochim. Acta*, vol. 53, pp. 1209-1221, 1988
[20] R. Bodnar, "Revised equation and table for determining the freezing point depression of H2O–NaCl solutions. Geochim," *Cosmochim. Acta*, vol. 57, p. 683, 1993.
[21] T. J. Shepherd, A. H. Rankin, and D. H. M. Alderton, "A practical guide to fluid inclusion studies, blackie, Glasgow and London," pp. 239. 1985.
[22] B. Mishra and M. K. Panigrahi, "Fluid evolution in the kolar gold field: Evidencefrom fluid inclusion studies," *Mineralium Deposita*, vol. 34, pp. 173-181, 1999.
[23] R. W. Hutchinson, "A multistage multiprocess genetic hypothesis for green stone hosted gold deposists," *Ore Geol. Rev*., vol. 8, pp. 349-382, 1993.
[24] D. I. Groves and R. P. Foster, "Archaean lode gold deposists," *Gold metallogeny and Exploration*, Chapman and Hall, London, pp 63-103, 1993.
[25] J. J. Wilkinson, "Fluid inclusions in hydrothermal ore deposists," vol. 55, pp. 229-272.

Grish Kumar Mayachar presently working as a mineralogist Sr. in NCEGR, Geological Survey of India, Bangalore. He did M,Sc, from Bangalore University and Ph. D. from University of Lucknow in 2008. He joined as a Mineralogist in Geological survey of India from 2008 and carried many RP (Research Projects) items of Gold and Copper in Archean terrains, especially in Southern India and tungsten projects from Central and Western India.